Analytical Theory of Ion-Temperature-Gradient Instability*

Shi-chong Guo and Jie-wu Shen

Institute of Physics, Academia Sinica

PPPL--1868

DE82 011307

Liu Chen

Plasma Physics Laboratory, Princeton University

Princeton, New Jersey 08544

S. T. Tsai

Institute of Physics, Academia Sinica

translated by

S. T. Tsai and L. Chen

ABSTRACT

The relationship between the threshold values of ion-temperature-gradient instabilities and the temperature parameters of plasmas is investigated analytically in slab and toroidal geometries separately. It is found that the threshold values increase rapidly when the ion temperature becomes much higher than the electron temperature. The change of the threshold values with respect to the ion temperature is quite similar for both geometric models. This finding is consistent with PLT observations. Furthermore, the analytical results also agree with those of the numerical calculations.

*Accepted for publication in Acta Physica Sinica.

I. INTRODUCTION

In *PLT* experiments with intense neutral beam heating, enhanced density fluctuations have been observed when ion temperature T_i becomes higher than a certain value, typically, $T_i \gtrsim 4$ KeV [1]. It has been suggested that these fluctuations may be due to drift instabilities driven by the ion temperature gradient. Recent PLT experiments, however, show that the enhanced fluctuations tend to disappear as T_i is further increased to $T_i \gtrsim 7$ KeV [2]. These observations thus suggest that, if the density fluctuations are indeed due to ion temperature gradient instability (here, we shall term it as the η_i mode with $\eta_i \equiv d \ln T_i / d \ln N_i$ characterizing the ion temperature gradient), the threshold value of the η_i mode may be closely related to the ion temperature. This problem has previously been investigated by numerical methods [3]. The purpose of the present work is to derive analytically the threshold (critical) η_i, η_{ic}, as a function of both $\tau \equiv T_e/T_i$ and $b_s/\tau = k_\theta^2 \rho_i^2/2$ (where ρ_i is the ion Larmor radius and k_θ is the poloidal wavenumber).

Since for the η_i mode ion kinetic effects play crucial roles in determining η_{ic}, kinetic equations are employed in this work, and ion Landau damping is included here as the collisionless dissipation mechanism. In Sec. II, analytical expressions for η_{ic} and the corresponding frequency Ω_r are derived for a slab plasma with finite magnetic shear. The analyses are then further extended to toroidal geometries in Sec. III. In Sec. IV, we compare the analytical results with those of numerical calculations. Finally, a brief summary and discussion are given in Sec. V.

We find that the analytical and numerical results are in reasonably good agreement. Both results indicate a sharp increase in η_{ic} as $T_i >> T_e$. Furthermore, the dependence of η_{ic} on τ is similar for both the slab and toroidal geometries. This finding provides us with a qualitative interpretation of the PLT experimental results. Meanwhile, we note that our description of the η_i mode based on the strong ballooning approximation [3] is also consistent with experimental observations [2].

II. SLAB MODEL

A. Eigenmode Equation. In the slab model, we assume the plasma inhomogeneities in density and temperature to be in the x direction. The equilibrium magnetic field is given by $\underset{\sim}{B} = B_o(\underset{\sim}{e}_z + \underset{\sim}{e}_y x/L_s)$ and B_o = const. The perturbed quantities, meanwhile, can be expressed as

$$\hat{\phi} = \phi(x)\ \exp[i(k_y y - \omega t)] \ .$$

The corresponding eigenmode equation for the η_i mode is then derived using the standard scheme via the gyrokinetic equation [4]. Furthermore, we have ignored, in the slab model, the magnetic-gradient drift and assume $k_\perp^2 \rho_i^2 \ll 1$ (i.e., ion Larmor radius being much smaller than the perpendicular wavelength) in deriving the perturbed ion density. Meanwhile, since the η_i mode is associated with the ion drift wave, the nonadiabatic electron contribution is negligibly small, and hence the electron density response can be taken to be Boltzman. Employing the quasi-neutrality condition, we obtain the following eigenmode equation:

$$\left(\frac{d^2}{dt^2} + Q(t,\Omega)\right)\phi(t) = 0, \tag{2.1}$$

where

$$Q = -b_s + \tau \frac{\tau+1 + (\tau+1/\Omega - \eta_i/2\Omega)Z_i\xi_i + (\eta_i/\Omega)\xi_i^2(1+Z_i\xi_i)}{(\tau + 1/\Omega + \eta_i/2\Omega)Z_i\xi_i + (\eta_i/\Omega)\xi_i^2(1+Z_i\xi_i)} ,$$

$$t = x/\rho_s\ , \quad \rho_s^2 = \rho_i^2\tau/2\ , \quad \tau = T_e/T_i\ , \quad b_s = k_y^2\rho_s^2\ ,$$

$$\Omega = \omega/\omega_{*e}\ , \quad \xi_i = -t_i/|t|\ , \quad t_i = -\ \Omega(\tau/2)^{1/2}(L_s/L_n)\ , \quad \omega_{*e} = k_y v_{Te}^2/2L_n\Omega_{ce}\ ,$$

v_T is the thermal velocity, Z is the plasma dispersion function, and L_n and L_s are, respectively, the scale lengths of the plasma density and the sheared magnetic field. Ω_c is the Larmor frequency, k is the wave number, ω is the mode frequency, and the subscripts i and e stand for ions and electrons, respectively.

B. Results of the Fluid Approximation. First we describe the solution of the eigenmode equation with the fluid-ion approximation ($|\omega/k_\parallel v_{Ti}|^2 >> 1$), and then we discuss the situation after the introduction of the kinetic effects.

Under the fluid approximation, Eq. (2.1) becomes

$$\left(d^2/dt^2 + Q_o - L_n^2(A-1)t^2/L_s^2\Omega^2\right)\phi(t) = 0, \tag{2.2}$$

where

$$Q_o = -b_s + \tau(1-\Omega)/(\Omega\tau+1+\eta_i)\ , \tag{2.3}$$

and

$$A = (1-\Omega)(\Omega\tau+1+2\eta_i)/(\Omega\tau+1+\eta_i)^2\ . \tag{2.4}$$

Equation (2.2) is a standard Weber equation. The eigenvalue condition then yields the following dispersion relation:

$$-\Omega[\tau(1-\Omega)/(\Omega\tau+1+\eta_i) - b_s] = (2n+1)(L_n/L_s)(A-1)^{1/2};\ n = 0,1,2,\ldots \quad . \tag{2.5}$$

We note that in Eq. (2.5) $b_s \sim L_n/L_s \ll 1$. For $\tau \gg b_s$ we recover the previous fluid result [5],

$$\Omega \approx i(L_n/L_s\tau)(1+\eta_i)(1-A)^{1/2} \ . \tag{2.6}$$

This is an unstable solution and $|\Omega| \ll 1$. For $\tau < 2b_s$, there is a marginally stable root with $|\Omega| \gg 1$. By using the perturbation method, we find, letting

$$\Omega = \Omega_o + \Omega_1 \ , \tag{2.7}$$

that

$$\Omega_o = \frac{-b_s(1+\eta_i)}{\tau(1+b_s)} \ , \tag{2.8}$$

and

$$\Omega_1 = \frac{1}{1+b_s} + (2n+1)\,\frac{L_n}{L_s\tau}\,\frac{(\Omega_o\tau+1+\eta_i)(A-1)^{1/2}}{[\Omega_o + 1/(1+b_s)](1+b_s)} \ . \tag{2.9}$$

Both solutions satisfy the conditions of the fluid-ion approximation so long as $\eta_i \gg 1$.

C. <u>The Threshold Value of the Instability and the Corresponding Eigenfrequency.</u>

(1) For $\tau < 2b_s$, the η_i mode is marginally stable in the fluid limit. The instability properties are completely determined by the kinetic effects. Using the large argument expansion for the plasma dispersion function in Q but retaining the imaginary part, we have

$$Q = Q_r + iQ_i \quad , \tag{2.10}$$

$$Q_r \simeq Q_o + (\tau/2\xi_i^2)(1-A), \text{ and } Q_i \simeq \tau[(a-b)c/b^2]\sqrt{\pi}\ \xi_i^3 \exp(-\xi_i^2) \quad ,$$

where

$$a = 1 - 1/\Omega \ , \quad b = -(\tau + 1/\Omega + \eta_i/\Omega) \ , \quad c = - \eta_i/\Omega \ ,$$

$$\Omega = \Omega_r + i\Omega_i \ , \text{ and } |\Omega_i| \ll |\Omega_r| \ .$$

One can easily see that $|Q_i| \ll |Q_r|$ and Q_r is the Q function under the fluid-ion approximation. Treating Q_i perturbatively, we find $\Omega_i > 0$ as $(a-b) < 0$ and $\Omega_i < 0$ as $(a-b) > 0$. Thus, the marginal stability condition $\Omega_i = 0$ can only exist at a = b, and we obtain

$$\eta_{ic} = -\Omega(1+\tau). \tag{2.11}$$

Letting

$$\eta_{ic} = \eta_o + \eta_1 \ , \tag{2.12}$$

we have

$$\eta_o = -\Omega_o(1+\tau) \; ; \quad \eta_1 = -\Omega_1(1+\tau) \; . \tag{2.13}$$

From Eqs. (2.8) and (2.13), we get

$$\Omega_o = -\frac{b_s}{\tau - b_s} \; ,$$

and

$$\eta_o = \frac{b_s}{\tau - b_s}(1+\tau) \; . \tag{2.14}$$

Using Eqs. (2.7), (2.9), (2.12), (2.13), and (2.14) one can solve for $\eta_{ic}(b_s,\tau)$ and the corresponding $\Omega_r(b_s,\tau)$. We plot η_{ic} and Ω_r versus τ in Figs. 1 and 2 (see curves A), respectively. It is clear that $\eta_{ic} \to \infty$ as τ approaches b_s. This means the η_i mode becomes more stable as ion temperature increases.

(2) For $\tau \gg b_s (b_s \sim L_n/L_s)$, the η_i mode is a purely growing mode in the fluid-ion approximation. Only the ion Landau damping can be a stabilizing factor. Obviously, the marginal stability can no longer be described by the fluid theory. We have to consider the case with $|\omega/k_\parallel v_{Ti}| \lesssim 1$.

We will apply the WKB approximation method to evaluate η_{ic} and Ω_r. First of all, the fluid theory gives us the following ordering, i.e., $\eta_{ic} \sim O(1)$ and $|\Omega\tau| \sim O(L_n/L_s) \ll 1$. Because the η_i mode is associated with the ion drift branch, Ω_r should be negative. (Numerical calculations have already shown this.)

We let the function $Q(t,\Omega)$ be analytically continued to the complex t-plane. Due to the symmetry in Q we need only to consider the right half plane. Let $z = 1/\xi_i = t/t_i$ and Re $z > 0$. For $|z| \ll 1$, we have

$$\Omega \simeq \Omega_o , \tag{2.15}$$

and

$$Q \simeq a_1/a_o + i[a_2 - \tau(\tau+1)z^2]/a_o z \; ; \quad \text{for } |z| \gg 1 , \tag{2.16}$$

where

$$a_o = -\sqrt{\pi}\,(1/\Omega + \eta_i/2\Omega + \tau),$$

$$a_1 = -\sqrt{\pi}\,[(\tau-b_s)(\tau+1/\Omega) - (\tau + b_s)(\eta_i/2\Omega)],$$

and

$$a_2 \simeq 2(\tau + 1/\Omega - \eta_i/\Omega)\tau . \tag{2.17}$$

Since the ion Landau damping is very important for reaching marginal stability, the turning points $\pm z_o$ can be expected to be in the strong damping regions; i.e., $|z_o| \gg 1$. Therefore, z_o can be obtained from Eq. (2.16). Meanwhile, the WKB numerical calculations indicate that the turning points lie very close to the real axis (i.e., $|z_{or}|^2 \gg |z_{oi}|^2$). Thus, we assume $4\tau(\tau + 1)a_2 \gg a_1^2$ and obtain

$$z_{or} \simeq [a_2/\tau(\tau+1)]^{1/2} \; ; \quad z_{oi} \simeq -a_1/2\tau(\tau+1) . \tag{2.18}$$

Here we note $z_{or} > 0$. Letting $s = z/z_o$, the WKB quantization condition gives

$$2t_i z_o \int_o^1 Q^{1/2}(\Omega,s)\, ds = (n + 1/2)\pi . \tag{2.19}$$

Noting that the real axis is in the subdominate region, the eigensolution is physically meaningful.

To carry out the integration in Eq. (2.19), we have to know $Q(\Omega,s)$ in the domain $0 \leq s \leq 1$. As suggested by the numerical results, we can join the two asymptotic values of Q function [i.e., Eqs. (2.15) and (2.16)] by the following simple relation

$$Q = \begin{cases} Q_o & , \text{ for } 0 \leq s < s_o \equiv 1/|z_o| \\ Q_R + i\, Q_i, & \text{for } s_o \leq s \leq 1 \end{cases} \quad ;$$

$$Q_R = Q_o(1-s)/(1-s_o); \quad Q_i = a_2(1-s^2)/a_o z_{or} s. \tag{2.20}$$

The real part of Eq. (2.19) gives

$$\Omega_r = \Omega_o/(1+s_o/2)^2, \tag{2.21}$$

$$\Omega_o = -(n+1/2)^2\pi^2(9/8)(L_n/L_s)^2(\tau+1)(1+\eta_i)/\tau\eta_i[\tau-b_s(1+\eta_i)] \ . \tag{2.22}$$

From Eqs. (2.18) and (2.21), we obtain

$$s_o = [1/2(1+3/4\alpha)]\{\alpha + [\alpha^2 - 4\alpha(1+3/4\alpha)]^{1/2}\} \quad ; \tag{2.23}$$

here, $\alpha = \Omega_o(\tau+1)/\eta_i$. The imaginary part of Eq. (2.19) gives

$$\eta_{ic} = \eta_o + \eta_1 \quad , \tag{2.24}$$

where

$$\eta_o = 2(\tau-b_s)/(\tau+b_s) \quad ,$$

and

$$\eta_1 = (3/\sqrt{\pi})[a_2\Omega_r\tau(\tau+1)/Q_o(1+s_o/2)(\tau+b_s)]\{(2/3)(1-s_o)^2-2(1-s_o)-(1-s_o)^{1/2}\ln$$

$$|[(1-s_o)^{1/2}-1]/[(1-s_o)^{1/2}+1]|\} + \eta_o\Omega_r\tau \; .$$

The above results of η_{ic} and Ω_r are plotted in Figs. 1 and 2 (see curves B). One can see that for $\tau >> b_s$ and L_n/L_s , η_{ic} depends weakly on τ.

(3) For $\tau \approx 2b_s$, the turning points are roughly located at 1 ($|z_o| \approx 1$), namely, $|\omega/k_\parallel v_{Ti}| \sim 1$. The methods used in cases (1) and (2) are no longer applicable. Hence, in order to investigate the properties of the η_i mode in this parameter regime, we can only make rough estimates on η_{ic} based on some known conditions. Numerical results indicate that the turning points are still close to the real axis at marginal stability. Therefore, we assume $z_o \approx 1$. It follows that the ion plasma dispersion function is given by $Z_i(-1,0) = Z_R + iZ_I$ and $Z_R \approx 1$. Since we know that at the turning points both the real and imaginary parts of Q must vanish and $|\Omega\tau| << 1$, the requirement of $Q_i = 0$ at $z = z_o$ yields

$$\eta_{ic} = \{-(3/2)\Omega(\tau+1)+[(9/4)\Omega^2(\tau+1)^2 - 4\Omega(\tau+1)]^{1/2}\}/2. \qquad (2.25)$$

From $Q_r = 0$ at $z = z_o$, we get

$$\tau/b_s \approx \frac{(1+\eta_i/2)^2 + Z_I^2(1+3\eta_i/2)^2}{Z_I^2(1+\eta_i/2)(1+3\eta_i/2) - (\Omega-1 + \eta_i/2)(1+\eta_i/2)} \; . \qquad (2.26)$$

The WKB quantization condition then gives

$$\Omega^3 - \Omega^2 \left[1-b_s(1+\eta_i)/\tau\right] = - h(1+\eta_i) \quad ,$$

and

$$h = (n+1/2)^2 \pi^2 L_n^2/2L_s^2\tau^2 \ . \tag{2.27}$$

Let $b_s = 0.2$ and $|\Omega + 1| << 1$, Eqs. (2.25) - (2.27) give $\Omega_o \simeq - 0.7$, $\eta_o \simeq 1.5$ and $\tau/b_s \simeq 1.9$. The slopes of the curves η_{ic} and Ω_r versus τ in this regime can also be obtained by perturbation about $z_o \simeq 1$. The results are shown by curves C in Figs. 1 and 2.

III. TOROIDAL CONFIGURATION

A. Eigenvalue Equation. For toroidal geometries, we adopt the coordinates (r, θ, ζ), where r is the minor radius, θ is the poloidal angle and ζ is the toroidal angle. We assume concentric, circular magnetic surfaces, and the magnetic field is given by

$$\underset{\sim}{B} = B(\underset{\sim}{e}_\zeta + \varepsilon/q\ \underset{\sim}{e}_\theta) \ , \quad B = B_o(1 - \varepsilon \cos\theta) \quad ,$$

where $q = rB_T/RB_p$ is the safety factor, $\varepsilon = r/R_o << 1$ and R_o is the major radius. The perturbed quantities can be expressed as

$$\phi(r,\theta,\zeta,t) = \tilde{\phi}(r,\theta)\exp[i(m_o\theta - n\zeta - \omega t)] \ ,$$

$$\tilde{\phi}(r,\theta) = \sum_j \hat{\phi}(j,r)\exp(ij\theta) \ .$$

The corresponding η_i mode eigenmode equation has been derived previously [3], and hence we only present the results in Eq. (3.1). The derivation itself is similar to that in the slab model, that is, it is based on the gyrokinetic equation with the toroidal effects manifested through the magnetic curvature- and gradient-drift terms. Furthermore, the ballooning-mode approximation is employed to reduce the two-dimensional problem to (in the zeroth-order approximation) a one-dimensional problem. The so-called Taylor's strong-coupling approximation is then used to simplify the one-dimensional difference equation to the following differential equation:

$$\{d^2/dt^2 + Q_T(\Omega,t)\}\phi(t) = 0 \; , \tag{3.1}$$

$$Q_T = (L_1 - L_2)/\{1 - (1/2 - \hat{s})L_2/(b_s\hat{s}^2)\} \; ,$$

where

$$L_1 = G\tau - b_s \; , \qquad L_2 = (2\varepsilon_n/\Omega)\xi_i^2 G_2 \; ,$$

$$G = (1 + 1/\tau + N_1D_1 + N_2D_2)/A_1 \; ,$$

$$N_1 = 1 + 1/\Omega\tau - 3\eta_i/2\Omega\tau \; , \qquad N_2 = \eta_i/\Omega\tau \; ,$$

$$D_1 = \xi_i Z_i \; , \qquad D_2 = \xi_i^2(1 + \xi_i Z_i) + \xi_i Z_i \; ,$$

$$A_1 = N_1D_1 + N_2(D_1 + D_2) \; , \qquad B_1 = N_1D_5 + N_2D_6 \; ,$$

$$G_2 = \left((B_1/A_1)(1 + 1/\tau) + N_1D_3 + N_2D_4\right)/A_1 \ ,$$

$$D_3 = B_1D_1/A_1 - D_1 + 2\xi_i^2(1 + D_1) \ ,$$

$$D_4 = B_1D_2/A_1 - D_2 + \xi_i^2\left(1 + 2\xi_i^2(1 + D_1)\right) \ ,$$

$$D_5 = -1 - 2\xi_i^2(1 + \xi_i Z_i) \ ,$$

$$D_6 = -5/2 - \xi_i^2(3 + 2D_1) - 2\xi_i^4(1 + D_1) \ ,$$

$$b_s = k_\theta^2\rho_s^2 \ , \quad \rho_s^2 = \rho_i^2\tau/2 \ , \quad \tau = T_e/T_i \ , \quad \Omega = \omega/\omega_{*e} \ , \quad \epsilon_n = r_n/R_o ,$$

$$\xi_i = -t_i/|t| \ , \quad t_i = -(q/\epsilon_n\hat{s})\Omega(\tau/2)^{1/2} \ , \quad t = z\Delta r_s/\rho_s \ , \quad z = s-j \ ,$$

$s = (r-r_o)/\Delta r_s$, $\Delta r_s = 1/k_\theta\hat{s}$, $\hat{s} = r_oq'/q$, $m_o = nq(r_o)$, $\omega_{*e} = k_\theta v_{Te}^2/2r_n\Omega_{ce}$. Here r_n is the density scale length in the radial direction, L_1 is the Q function of the slab model, and the rest of the notation is the same as that stated in Sec. II.

B. The Lowest-Order Eigenvalue. Due to the comple ity of the toroidal case, we have to rely more on the information provided by numerical calculations. From numerical calculations, we know that in the parameter region which we are interested in there always exists a solution with turning points in the domain $|z_o| < 1$, i.e., $|\omega/k_\parallel v_{T_i}| > 1$. In this regime, the kinetic effect is very weak. We therefore can follow the method used in treating the $\tau<2b_s$ case in the slab model, i.e., we treat the kinetic effect as a first-order correction to the zeroth-order solution obtained with the fluid approximation.

In the large argument expansion, the function $Q_n(t,\Omega)$ becomes, keeping $O(\xi^{-2})$ terms,

$$L_1 = Q_o + \tau(1-A)/2\xi_i^2 \ , \quad L_2 = (2\varepsilon_n/\Omega)(1 - 3A/2 + B/2\xi_i^2) \quad ,$$

where

$$A = (1-\Omega)(\Omega\tau+1 + 2\eta_i)/(\Omega\tau+1 + \eta_i)^2,$$

$$B = 3\,\frac{1-\Omega}{\Omega\tau+1 + \eta_i}\,\frac{(\Omega\tau+1 + 2\eta_i)^2}{(\Omega\tau+1 + \eta_i)^2} - \frac{15}{2}\,\frac{(\Omega\tau+1+ 3\eta_i)}{(\Omega\tau+1 + \eta_i)^2} + \frac{7}{2}\,\frac{\Omega\tau+1 + 2\eta_i}{\Omega\tau+1 + \eta_i} \ ,$$

$$Q_o = \frac{(1-\Omega)\tau}{\Omega\tau + 1 + \eta_i} - b_s .$$

The simplified eigenmode equation can be written as

$$\left(d^2/dt^2 + (Q_o - \Delta)/(1+C\Delta) - \tau\, D/2\xi_i^2\right)\phi(t) = 0 \quad , \qquad (3.2)$$

where

$$\Delta = (2\varepsilon_n/\Omega)(1-3A/2) \ , \quad C = (\hat{s} - 1/2)/(b_s \hat{s}^2) \ ,$$

$$D = -\,\frac{1-A - 2\varepsilon_n B/\Omega\tau}{1+C\Delta} + \frac{(Q_o-\Delta)\,CB2\varepsilon_n/\Omega\tau}{(1+C\Delta)^2} .$$

Equation (3.2) can be solved to give the dispersion relation

$$-\,\Omega(Q_o-\Delta) = (2n + 1)(\hat{s}/q)\,\varepsilon_n D^{1/2}(1+c\Delta); \quad n = 0,\ 1,\ 2,\ \ldots \quad . \qquad (3.3)$$

In the following, we are going to use Eq. (3.3) to evaluate Ω in three different cases for the n = 0 eigenstate.

(1) For $\tau < 2b_s$, we have $|\Omega| >> 1$, $\eta_{ic} >> 1$, and $\Omega\tau \sim O(1)$. Since $|2\varepsilon_n/\Omega| << 1$, the toroidal correction is not important. Equation (3.3) gives

$$\Omega = \Omega_o + \Omega_1 , \tag{3.4}$$

$$\Omega_o = -b_s(1+\tau)/\tau(1+b_s) , \tag{3.5}$$

$$\Omega_1 = \frac{1}{1+b_s} + \frac{(\Omega_o\tau+1 + \eta_i)}{[\Omega_o+1/(1+b_s)](1+b_s)\tau}\left[\frac{\varepsilon_n\hat{s}}{q}(A-1)^{1/2}(1+C\Delta) + 2\varepsilon_n(1-3/2A)\right]. \tag{3.6}$$

One can see that, to the lowest order, it is the corresponding slab result. The toroidal correction is in the higher-order Ω_1 term.

(2) For $\tau >> 2b_s$, the numerical results tell us that this corresponds to the $|\Omega| << 1$, $\eta_{ic} \sim O(1)$, and $|\Omega\tau + 1| << 1$ cases. Since $|2\varepsilon_n/\Omega| \sim O(1)$, the toroidal correction is important, i.e., in the same order as the slab term. Equation (3.3) gives

$$\Omega_o = 2\varepsilon_n(\eta_i - 3)/(\tau - b_s\eta_i) , \tag{3.7}$$

$$\Omega_1 = -\frac{\eta_i\varepsilon_n}{2(\tau-b_s\eta_i)}\left[\frac{\hat{s}}{q}D^{1/2}(1+C\Delta)\right] . \tag{3.8}$$

This is still a marginally stable solution. Therefore, the toroidal effect can extend the marginally stable solution which, in the slab model, only exists for $\tau < 2b_s$ to the regime of $\tau >> 2b_s$.

(3) For $\tau > 2b_s$, we know that in this regime $|\Omega| \sim 1$ and $|\Omega\tau + 1| << 1$. Equation (3.3) then yields

$$\Omega_o = \frac{1}{2}\{(1 - \frac{b_s\eta_i}{\tau} - \frac{6\varepsilon_n}{\tau}) + [(\frac{b_s\eta_i}{\tau} - 1 + \frac{6\varepsilon_n}{\tau})^2 + 4\ (\frac{2\varepsilon_n}{\tau} - \frac{2\varepsilon_n\eta_i}{\tau})]^{1/2}\}\ , \tag{3.9}$$

$$\Omega_1 = (\frac{\hat{s}}{q}\ \varepsilon_n D^{1/2}(1+C\Delta)\ \frac{\eta_i}{\tau})/(\frac{b_s\eta_i}{\tau} - 1 + \frac{6\varepsilon_n}{\tau} + 2\Omega_o)\ . \tag{3.10}$$

C. Evaluation of η_{ic}. We now consider the ion kinetic effects by taking the large argument expansion of Z_i but retaining the imaginary part. Thus,

$$\Omega_T = \Omega_r + i\Omega_i$$

$$= \frac{\mathrm{Re}L_1 - \mathrm{Re}L_2}{1+C\mathrm{Re}L_2} - i\ \frac{C\mathrm{Re}L_1+1}{(1+C\mathrm{Re}L_2)^2}\ \frac{2\varepsilon_n}{\Omega}\ \frac{1}{(\mathrm{Re}A)^2}\ (1+\frac{1}{\tau}+\frac{\eta_i}{\Omega\tau}).$$

$$(\frac{-2\eta_i}{\Omega\tau})\sqrt{\pi}\ \xi_i^{-7}\exp(-\xi_i^2)\ . \tag{3.11}$$

Here, we only keep the leading imaginary terms which come from L_2, the toroidal contribution. Perturbation theory shows that the condition for obtaining a marginally stable solution ($\Omega_i = 0$) is $(1+ 1/\tau + \eta_i/\Omega\tau) = 0$, i.e.,

$$\eta_{ic} = -\ \Omega(1+\tau)\ . \tag{3.12}$$

Solving the simultaneous Eqs. (3.5), (3.7), (3.9), and (3.12), one can find the analytic expressions for η_o, Ω_o in terms of the parameters τ, b_s and ε_n.

(1) For $\tau < 2b_s$,

$$\Omega_o = -b_s/(\tau - b_s) ,$$

$$\eta_o = b_s(1+\tau)/(\tau-b_s) .$$

(2) For $\tau >> 2b_s$,

$$\Omega_o = \left([-2\varepsilon_n(\tau+1)-\tau] + \{[\tau+2\varepsilon_n(1+\tau)]^2 - 24\varepsilon_n b_s(1+\tau)\}^{1/2}\right)/2b_s(1+\tau) ,$$

$$\eta_o = \left(\tau + 2\varepsilon_n(1+\tau) - \{[\tau + 2\varepsilon_n(1+\tau)]^2 - 24\varepsilon_n b_s(1+\tau)\}^{1/2}\right)/2b_s .$$

(3) For $\tau > 2b_s$,

$$\Omega_o = \left\{-\left(\frac{\tau}{1+\tau} + 2\varepsilon_n - \frac{6\varepsilon_n}{1+\tau}\right) + \left[\left(\frac{\tau}{1+\tau} + 2\varepsilon_n - \frac{6\varepsilon_n}{1+\tau}\right)^2 - 24\frac{\varepsilon_n}{1+\tau}\left(b_s - \frac{\tau}{1+\tau}\right)\right]^{1/2}\right\}/$$

$$2[b_s-\tau/(1+\tau)] ,$$

$$\eta_o = -\Omega_o(1+\tau) .$$

As in the slab case, $\eta_{ic}(\tau,b_s)$ and the corresponding $\Omega_r(\tau,b_s)$ can be obtained by Eqs. (3.4) and (3.12). We plot the results on Figs. 3 and 4 as curves T.

D. <u>The Unstable Solution in the Fluid Approximation.</u> When $|\Omega| << 1$, $\eta_i >> 1$, and $|\Omega\tau| << 1$, Eq. (3.3) has another unstable solution

$$\Omega \sim 2\varepsilon_n(1-3A/2) + i(2n + 1)(\hat{s}/q)\varepsilon_n(-D)^{1/2}(1+C\Delta)(1+\eta_i)/[\tau-b_s(1+\eta_i)] ,$$

such that $\Omega_r \sim O(\varepsilon_n)$, and $\Omega_i \sim (\varepsilon_n/\tau)(1+\eta_i)$. This solution corresponds to the unstable fluid mode in the slab model. However, both analytic estimates and numerical calculations indicate that the corresponding η_{ic} is larger than those considered in C. Since we are only interested in the lowest threshold value, this branch of unstable mode will not be discussed in detail here. The dotted curve in Fig. 3 is the WKB numerical result.

IV. COMPARISON OF ANALYTICAL WITH NUMERICAL RESULTS.

We have used here two different numerical methods. One is a direct numerical solution of the eigenmode equation using the scheme described in Ref. 6. The results are plotted in Figs. 1 - 4 by the dot-dash lines. The second method is numerically solving the WKB quantization condition to obtain the eigenvalues. The results are plotted in Figs. 1 - 4 by the dash lines.

In the slab model, we have taken $b_s = 0.2$, $L_n/L_s = 0.1$, $\tau = 0.3 - 2.5$. In the toroidal model, we have taken, correspondingly, $b_s = 0.2$, $\varepsilon_n = 0.1$, $\hat{s} = \alpha = 1$ and $\tau = 0.3 - 2.5$. The plots show the dependence of η_{ic} and Ω_r on τ.

Analytic results are plotted on Figs. 1 - 4 as curves A, B, and C (for a slab) and curve T (for a torus). They are in good agreement with the numerical results both qualitatively and, in most domains, quantitatively. For the slab model, curves A and B do not fit well around $\tau = 0.4$. This is expected because both approaches break down near $|z_o| \sim 1$. Other discrepancies may be due to either the fact that we only retain the lowest order terms of Ω_i or the fact that the small parameters which we have used in the perturbation expansion are in fact not small enough. In any case, since the physics most interesting to us is the qualitative behavior of η_{ic} , results from the lowest-order approximation are sufficiently satisfactory.

V. SUMMARY AND DISCUSSION

In this work, the dependence of the threshold values of the η_i mode, η_{ic}, on the plasma temperature parameter τ is investigated for both slab and toroidal configurations.

(1) In the slab model with $\tau < 2b_s$, the η_i mode is marginally stable ($\Omega_i = 0$) under the conditions of the fluid approximation. Its stability property is solely governed by the ion Landau damping effect. We have found that the threshold value η_{ic} is much larger than unity and increases sharply as τ approaches b_s. In the regime $\tau \gg b_s$, the η_i mode is almost a purely growing mode in the fluid approximation and can be stabilized by the effect of ion Landau damping only. The threshold value η_{ic} is of order unity and is insensitive to the parameter τ for $\tau > 1$.

(2) In toroidal plasmas, the relation between η_{ic} and τ is similar to that in the slab model. For $\tau < 2b_s$, the toroidal correction is only of higher order; hence, in the lowest order, the solution is the same as that in the slab geometry. When $\tau \gg b_s$, the toroidal effect becomes important and its physical mechanism is entirely different from the slab model although the magnitude of the threshold value in both geometries are quite close.

In toroidal geometries, the marginally stable η_i mode is obtained in the fluid approximation. The corresponding η_{ic} is thus determined by the ion kinetic effects. We also find the existence of an unstable solution (similar to the $\tau \gg 2b_s$ case in the slab model) which, however, has higher η_{ic}.

(3) For various regimes of parameters, the results we have obtained by both analytical and numerical methods are in good agreement at least qualitatively. This is particularly clear in that η_{ic} increases sharply as τ is reduced for a fixed b_s. Thus, under conditions such that the instability of the η_i mode exists, if the ion temperature increases rapidly with the

electron temperature being maintained nearly constant and the value of η_i increases more slowly than η_{ic} does it will lead to the stabilization of the η_i mode. This conclusion is consistent with the experimental observations in PLT [2]. In addition, we find in our theoretical calculations that the strong ballooning approximation is a good approximation for the η_i mode [3]. This is also consistent with the experimental observation in which the detected fluctuations have ballooning structure [2]. Based on the above two points, we believe that our theoretical results have provided a qualitative explanation of the PLT experimental results.

It is worthwhile to point out that when $\tau \simeq b_s$, $k_y^2\rho_i^2 \simeq 1/2$ [it is also known by numerical computations, that $k_x\rho_i \sim O(1)$ as $\tau \simeq b_s$] , our work has already reached its validity limit, beyond which the differential eigenmode equation is no longer applicable. Hence, more rigorous calculations have to be given by solving the integral eigenmode equation.

Acknowledgment

The authors would like to acknowledge Mr. S. J. Wong and Mr. C. Y. Zhan for their valuable discussion in the numerical calculations.

This work was supported by United States Department of Energy Contract No. DE-AC02-76-CHO3073.

References

(1) H. Eubank et al., in "Proceeding of the 7th International Conference on Plasma Physics and Controlled Nuclear Fusion Research," Innsbruck, Austria, 1978 (IAEA, Vienna, Austria 1979) Vol. 1 p. 167.

(2) W. Stodiek et al., in "8th International Conference on Plasma Physics and Controlled Nuclear Fusion Research," IAEA-CN-38/A-1, Brussels, Belgium, 1980.

(3) P. N. Guzdar, L. Chen, W. M. Tang, and P. H. Rutherford. PPPL Report 1601 (1980). The translators note that the strong ballooning (coupling) approximation was first introduced by J. B. Taylor in a 1977 IAEA publication.

(4) For example, see W. M. Tang, Nuclear Fusion, 18, 1089 (1978).

(5) B. Coppi, M. N. Rosenbluth, and R. Z. Sagdeev, Phys. Fluids, 10, 582 (1967).

(6) T. Watanabe et al., Institute for Fusion Theory, Hiroshima University Research Report, Hift-23 (1980).

Figure Captions

Figure 1. Plot of η_{ic} versus τ for the slab model. The solid, dashed, and dot-dashed lines correspond, respectively, to analytic, numerical WKB, and direct numerical (shooting) results.

Figure 2. Plot of Ω_r versus τ for the slab model. The rest is the same as in Fig. 1.

Figure 3. Plot of η_{ic} versus τ for the toroidal configuration. The short dashed line corresponds to the η_{ic} of the branch which is unstable in the fluid approximation (c.f. Sec. III). The rest is the same as in Fig. 1.

Figure 4. Plot of Ω_r versus τ for the toroidal configuration. The rest is the same as in Fig. 3.

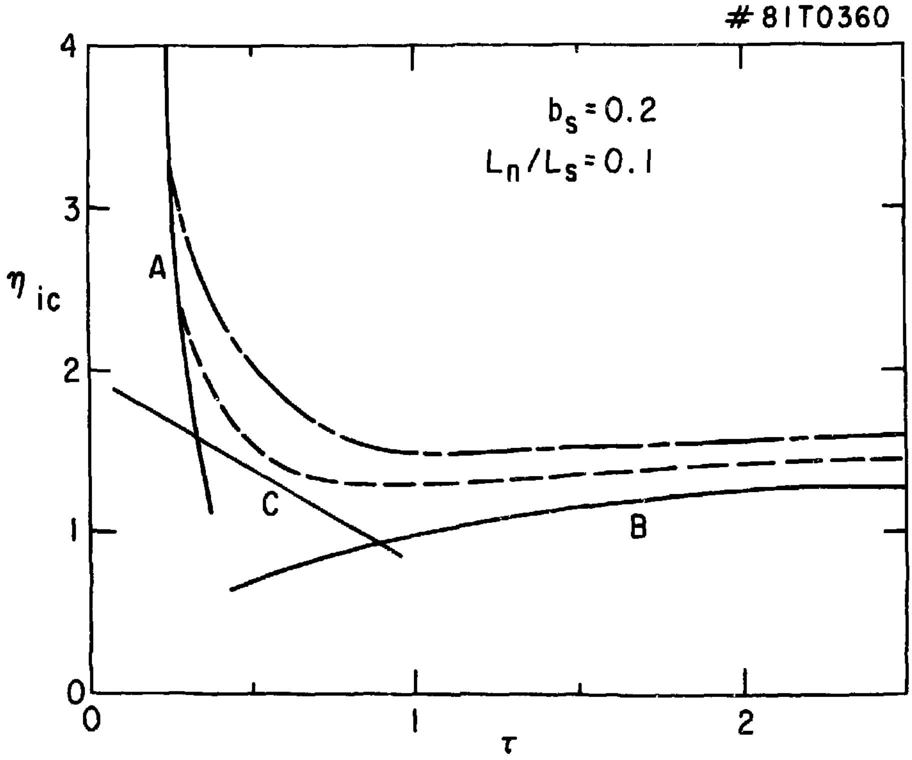

Fig. 1

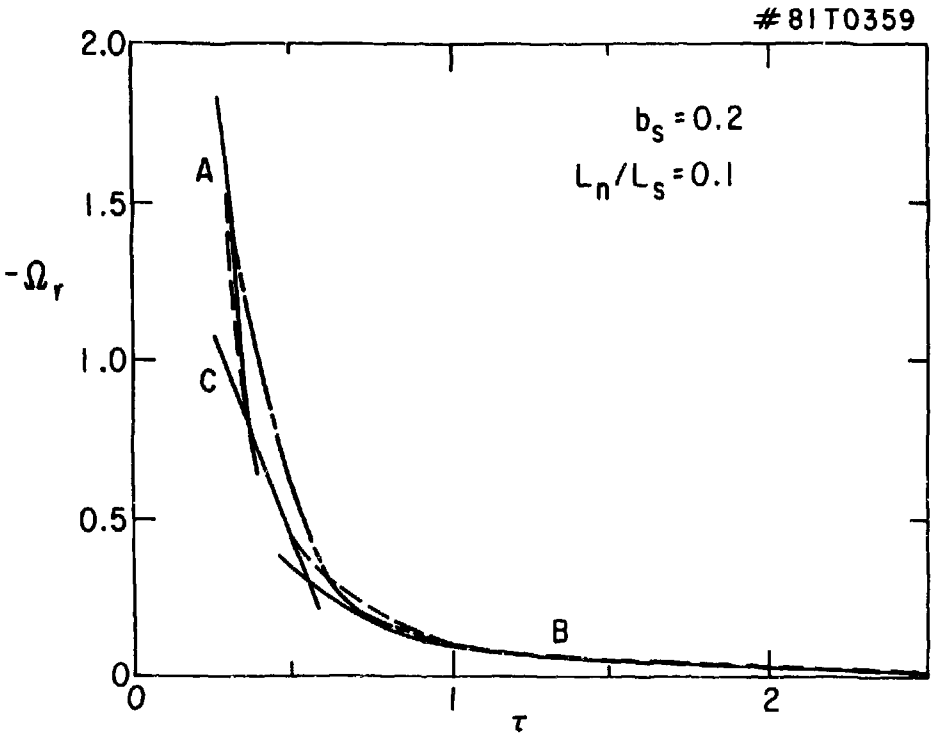

Fig. 2

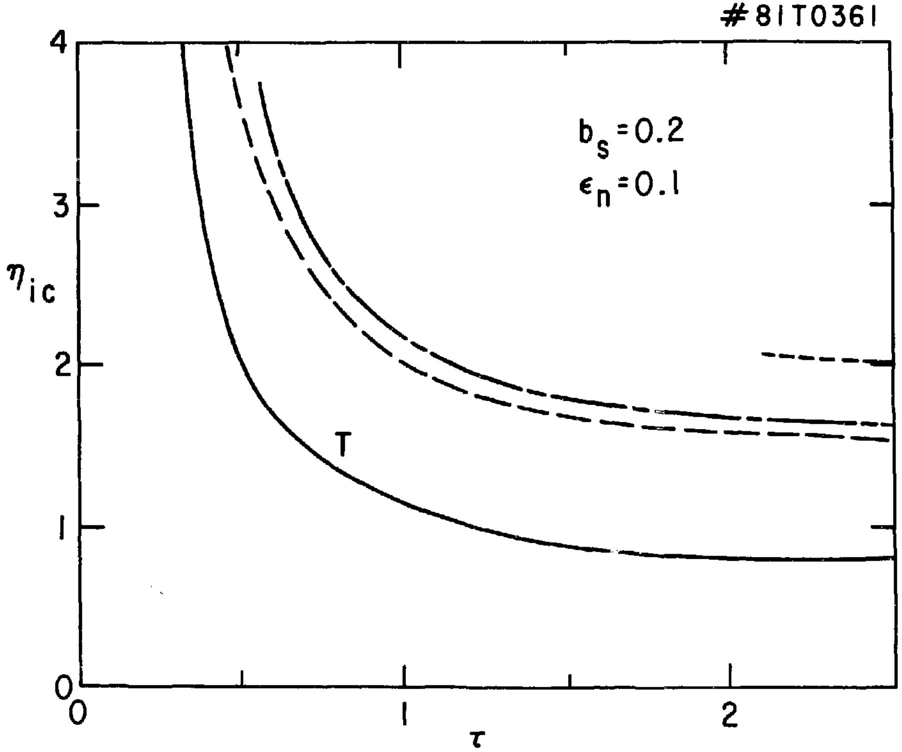

Fig. 3

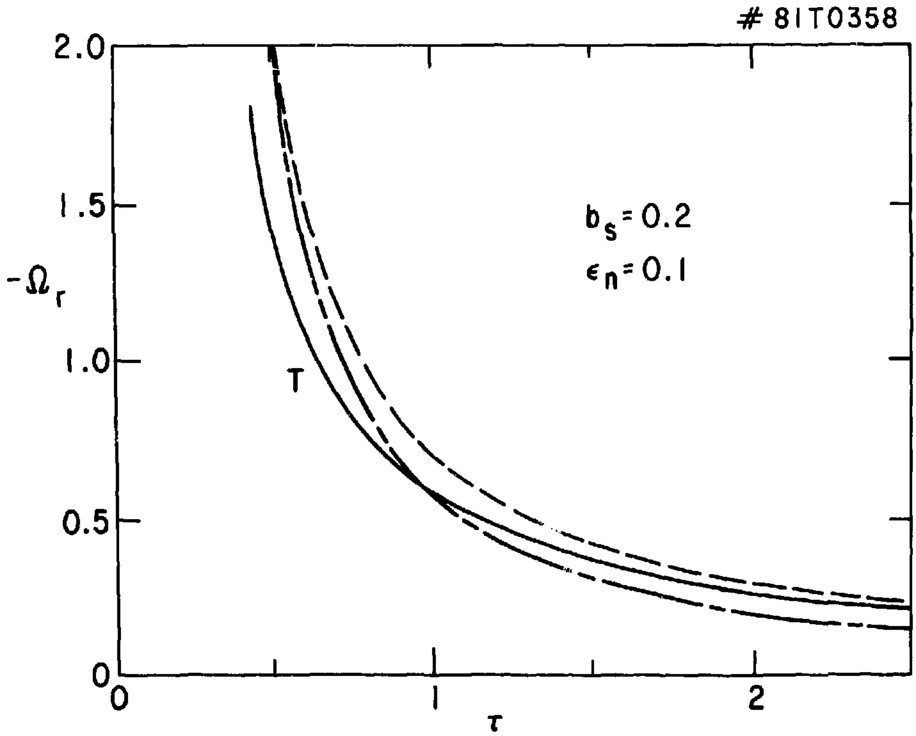

Fig. 4